Water Resources Research

RESEARCH ARTICLE
10.1029/2023WR034690

Effects of Snow Water Storage on Hydrologic Partitioning Across the Mountainous, Western United States

K. E. Hale[1,2,3], K. N. Musselman[1,2], A. J. Newman[4], B. Livneh[5,6], and N. P. Molotch[1,2,7]

[1]Department of Geography, University of Colorado Boulder, Boulder, CO, USA, [2]Institute of Arctic and Alpine Research, University of Colorado Boulder, Boulder, CO, USA, [3]Department of Civil and Environmental Engineering, University of Vermont, Burlington, VT, USA, [4]Research Applications Laboratory, National Center for Atmospheric Research, Boulder, CO, USA, [5]Cooperative Institute for Research in Environmental Science, University of Colorado Boulder, Boulder, CO, USA, [6]Department of Civil, Environmental, and Architectural Engineering, University of Colorado Boulder, Boulder, CO, USA, [7]Jet Propulsion Laboratory, California Institute of Technology, Pasadena, CA, USA

Abstract In the montane western United States, where the majority of downstream water resources are derived from snowmelt, a warming climate threatens the timing and amount of future water availability. It is expected that the fraction of precipitation falling as snow will continue decreasing and the timing of snowmelt will continue shifting earlier in the year with unknown impacts on partitioning between evapotranspiration and streamflow. To assess this, we employ a Snow Storage Index (SSI) to represent the annual temporal phase difference between daily precipitation and daily modeled surface water inputs (SWI, the sum of rainfall and snowmelt), weighted by the respective amounts. We coupled the SSI metric with a Budyko-based framework to determine the effect of snow water storage on relative hydrologic partitioning across snow-influenced watersheds in the western U.S. Greater snow water storage was positively correlated with greater hydrologic partitioning to streamflow, particularly in the North Cascades/Cascades (r^2: 0.62), Blue Mountains (r^2: 0.56), Canadian Rockies (r^2: 0.55), Idaho Batholith, (r^2: 0.48), and Columbia Mountains/Northern Rockies (r^2: 0.45). The weekly SWI:P ratio was an equally strong predictor for hydrologic partitioning, particularly in mid-spring (e.g., March/April) in the same mountainous areas (r^2: 0.62–0.74, across the same eco-regions). The retention of snow water storage and subsequent release of stored water in summer months resulted in increased hydrologic partitioning to streamflow. If SSI decreases with future warming, the volume of water partitioned streamflow will decrease non-uniformly across the western U.S. with substantial implications for ecosystems and agricultural, industrial, and domestic water supplies.

Key Points:

- Greater snow water storage is associated with greater partitioning of annual precipitation to streamflow
- Decreases in snow water storage with future warming will decrease streamflow volumes non-uniformly across the western United States
- Snow water storage metrics offer a basis to compare the temporal misalignment between snowfall and snowmelt

Supporting Information:

Supporting Information may be found in the online version of this article.

Correspondence to:

K. E. Hale,
khale1@uvm.edu

Citation:

Hale, K. E., Musselman, K. N., Newman, A. J., Livneh, B., & Molotch, N. P. (2023). Effects of snow water storage on hydrologic partitioning across the mountainous, western United States. *Water Resources Research*, *59*, e2023WR034690. https://doi.org/10.1029/2023WR034690

Received 16 FEB 2023
Accepted 5 JUL 2023

Author Contributions:

Conceptualization: K. E. Hale, K. N. Musselman, N. P. Molotch
Data curation: K. E. Hale, A. J. Newman, B. Livneh
Formal analysis: K. E. Hale
Funding acquisition: N. P. Molotch
Investigation: K. E. Hale, K. N. Musselman
Methodology: K. E. Hale, K. N. Musselman, N. P. Molotch
Project Administration: N. P. Molotch
Resources: K. N. Musselman, A. J. Newman, B. Livneh, N. P. Molotch
Supervision: N. P. Molotch

1. Introduction

Seasonal snowpack is an essential component of Earth's hydrological cycle, and about one-sixth of the global population relies on seasonal snowpack and glacier-derived runoff as a primary water resource (Barnett et al., 2005; Pörtner et al., 2019). Mountain snowpacks act as a natural "water tower," storing winter snowfall until it melts throughout spring and summer months, when downstream water demand is high (Foster et al., 2016; Immerzeel et al., 2020; Messerli et al., 2004). While many studies have investigated snowpack, snowmelt, and associated trends across spatial and temporal scales (e.g., Mote et al., 2018; Musselman et al., 2017, 2021), the comparative manner in which local to regional snowpacks store and release water has been relatively understudied. Snowmelt contributes to regional water supply and partially dictates the timing and amount of downstream water resources. Previous observed and model-based efforts have evaluated snowpack duration, snowmelt timing, rate, and associated implications (Alonso-González et al., 2022; Barnhart et al., 2020; Clow, 2010; Conway et al., 2021; Elias et al., 2021; Stewart et al., 2004). Yet one new method for evaluating snow water storage is via the daily temporal offset between the timing of precipitation and surface water inputs (SWI, daily the summation of rainfall and snowmelt) and their relative magnitudes, per year (Hale et al., 2023). Hydrologic metrics associated with this temporal delay can explicitly capture the mechanisms controlling the amount of downstream water availability that are also highly sensitive to climate change (Barnhart et al., 2016; Berghuijs et al., 2014; Foster et al., 2016; Jeton et al., 1996).

Climate warming has caused fundamental hydrologic changes with unknown and likely variable effects on water availability (Berghuijs et al., 2014; Foster et al., 2016; Gupta & Soroosh, 1998; Hinckley et al., 2012; Kapnick et al., 2018; Livneh & Badger, 2020; Safeeq et al., 2013). In the last century, there has been a gradual shift from

Validation: K. E. Hale, K. N. Musselman, A. J. Newman, B. Livneh, N. P. Molotch
Visualization: K. E. Hale, K. N. Musselman, A. J. Newman, B. Livneh, N. P. Molotch
Writing – original draft: K. E. Hale, N. P. Molotch
Writing – review & editing: K. E. Hale, K. N. Musselman, A. J. Newman, B. Livneh, N. P. Molotch

snowfall to rainfall (Knowles et al., 2006; Lute et al., 2015), decreases in peak snow water equivalent (SWE) (Mote et al., 2018), earlier onset of snowmelt (Musselman et al., 2017), and shorter snow cover duration in mountainous regions across the United States (U.S.) and globally (Brown & Mote, 2009; Brown & Robinson, 2011; Hammond et al., 2018; Stewart, 2009). In response to these changes, hydroclimatic studies have reported net decreases in annual streamflow and net increases in annual potential evapotranspiration (PET) associated with climate warming (Adam et al., 2006; Anghileri et al., 2016; Clow, 2010; Mahanama et al., 2012; McCabe & Clark, 2005; Regonda & Rajagopalan, 2004; Tang & Lettenmaier, 2012). A reduction in the annual fraction of total precipitation falling as snow (i.e., snowfall fraction) and earlier snowmelt timing directly effects the amount and temporal duration of snow water storage, which likely impacts the amount and timing of regional water availability (Barnhart et al., 2016; Cayan et al., 2001; Harpold et al., 2012; Stewart et al., 2004, 2005; Trujillo & Molotch, 2014; Trujillo et al., 2012). Cumulatively, these changes can adversely impact ecosystem function (Wieder et al., 2022) and may cause large deficits in agricultural, industrial and domestic water supplies (Griffin & Anchukaitis, 2014; Immerzeel et al., 2020; Yoon et al., 2015).

The manner in which climate warming erodes the distinct storage behavior of mountain snowpacks (Mote et al., 2018) and impacts hydrologic partitioning is an emerging knowledge gap. Recent work suggests that the snowfall fraction and snowmelt rate are closely related to streamflow partitioning across the contiguous United States (CONUS), with increased snowfall and higher snowmelt rates leading to greater proportional runoff (Barnhart et al., 2016; Berghuijs et al., 2014). Yet questions remain, including the physical mechanisms that govern hydrologic partitioning sensitivities to changes in snow water storage. Evaluating hydrologic partitioning in the context of snow water storage across climates in the western U.S. addresses this knowledge gap, as the seasonal cycles of precipitation (including the phase of precipitation), snowmelt, and PET are inherently linked with partitioning (Barnhart et al., 2016; Berghuijs et al., 2014; Clow, 2010; Foster et al., 2016; Hale et al., 2023; Harpold et al., 2012; Hu et al., 2010).

Two competing hypotheses in the recent literature exist regarding the effect of snow water storage on water partitioning to streamflow (Barnhart et al., 2016; Foster et al., 2016). The first hypothesis regards the role of snowpack water storage in controlling the timing and magnitude of water delivery to terrestrial systems. In this context, areas/years with relatively high snow water storage are associated with a relatively late and pronounced spring-summer snowmelt pulse (Musselman et al., 2017; Trujillo & Molotch, 2014). Hence, with a relatively large and rapid snowmelt pulse, SWI efficiently overwhelm soil moisture deficits and soil field capacity, leading to efficient streamflow production and greater partitioning to streamflow (Barnhart et al., 2016). Under this first hypothesis, a warming-related reduction in snow water storage, and the magnitude of this pronounced snowmelt pulse may reduce annual hydrologic partitioning to streamflow as a muted, earlier snowmelt pulse will be less efficient at generating soil drainage and sub-surface flow (Musselman et al., 2017).

The second hypothesis regards the role of snowpack water storage in creating a temporal alignment between SWI and PET (Foster et al., 2016; Jeton et al., 1996). Thus, a warming-induced shift from snowfall to rainfall, or toward earlier snowmelt, may diminish the temporal alignment of SWI and PET and increase cold-season hydrologic partitioning to streamflow (Foster et al., 2016; Hale et al., 2022; Hammond & Kampf, 2020) and decrease the amount of water available for evapotranspiration (ET) later in the year (Jeton et al., 1996; Robles et al., 2021). In opposition to the first hypothesis, reductions in snow water storage would act to increase hydrologic partitioning to streamflow. It is expected that these two contrasting hypotheses are simultaneously acting on catchment hydrology in snow-influenced areas, with varying sensitivities to warming. The degree to which one hydrologic partitioning sensitivity may dominate over the other is likely determined by complex interactions between the hydroclimatology and critical zone architecture of a given watershed (Brooks et al., 2015).

We quantify the effects of seasonal snowpack water storage and meltwater release on annual water partitioning in mountain headwaters of the western U.S. In this context, we evaluate the role of snowpack water storage, precipitation, SWI, and PET in terms of long-term runoff ratios and evaporative fractions using the Budyko framework (Budyko, 1974). The Budyko framework presents a hypothesis that predicts partitioning of incoming precipitation (P) between streamflow (Q), or ET based on an index of regional or catchment aridity (PET/P). Using existing and improved estimation of the magnitude and timing of snow water storage (Hale et al., 2023), we explicitly evaluate spatio-temporal patterns of snow water storage and associated climate sensitivities of hydrologic partitioning by addressing the question: *How does the timing and magnitude of snow water storage influence hydrologic partitioning across climates in the western United States?*

2. Methods

To evaluate the impact of snow water storage on hydrologic partitioning, we used a previously developed index of snow water storage (hereafter the Snow Storage Index (SSI); see Section 2.3 for description) that was derived by the difference in magnitude and timing of annual precipitation and the magnitude and timing of annual SWI (Hale et al., 2023). The index affords an explicit comparison of the volume and duration of water that is stored in the regional snowpack, and its effect on annual partitioning of water inputs to ET and streamflow (Q). Anomalies from expected hydrologic partitioning behavior were determined using the Budyko framework and were statistically evaluated in the context of the SSI (see Section 2.5) (Budyko, 1974).

2.1. Study Area

The study area includes the major mountainous U.S. Environmental Protection Agency, Level III eco-regions of the western U.S. (CEC, 2011). The average elevation of these eco-regions is 2,078 m, ranging from 638 to 3,857 m (CEC, 2011; Trujillo & Molotch, 2014), and include the following mountain ranges: North Cascades, Cascades, Sierra Nevada, Columbia Mountains/Northern Rockies, Blue Mountains, Idaho Batholith, Canadian Rockies, Middle Rockies, Wasatch and Uinta Mountains, and Southern Rockies. After constraining eco-regions to areas of with significant annual average snow water storage (annual average SSI > 0, see Section 2.3), the Eastern Cascades Slopes and Foothills, and Klamath Mountains were excluded from this analysis due to their relatively small areas and low grid-cell counts. The northern-most eco-regions have been evaluated only to the USA-Canada border, as observation-based hydrologic partitioning data, used to compare against the modeled data set (see Section 2.2), were only available across CONUS (Newman et al., 2015). Most corresponding hydrologic partitioning studies were also constrained to the western U.S. (Barnhart et al., 2016; Berghuijs et al., 2014; Mote et al., 2018).

The mountainous western U.S. stores considerable water in seasonal snowpack within two distinct climates: Maritime climate and a combination of inter-mountain and continental climates (Trujillo & Molotch, 2014). The maritime climates are associated with relatively warmer, drier conditions in summer months, and cooler, wetter conditions in winter months with a strong influence from atmospheric rivers (Cayan et al., 2001; Guan et al., 2010; Neiman et al., 2011; Regonda et al., 2005). Inter-mountain and continental climates are semi-arid with relatively colder winter temperatures, warmer summer temperatures, and thus greater annual temperature variability. These areas contain higher elevation mountain ranges, while experiencing plumes of moisture from the Pacific coast (Harpold et al., 2012; Kapnick & Hall, 2012; Mote et al., 2005; Wise, 2012). Within each climate (maritime vs. inter-mountain/continental), northern eco-regions tend to be more energy-limited (i.e., colder and wetter) and southern eco-regions tend to be more water-limited (i.e., warmer and drier) (Mote et al., 2005; Trujillo & Molotch, 2014). We used these differences in climates and relative energy or water limitations to group eco-regions into four classes: *maritime/more energy-limited* (Cascades and North Cascades), *maritime/more water-limited* (Sierra Nevada), *continental/more energy-limited* (Blue Mountains, Idaho Batholith, Canadian Rockies, Columbia Mountains/Northern Rockies), *continental/more water-limited* (Middle Rockies, Wasatch and Uinta Mountains, Southern Rockies). The framework used to differentiate these four groups of eco-regions is explained in Section 2.5.

2.2. Data Sets

We used a gridded hydrometeorological data set, which contains spatially and temporally continuous daily meteorological forcings and simulated Variable Infiltration Capacity (VIC) model states and fluxes at 1/16° (~6 km) resolution from 1950 to 2013 (Liang et al., 1994; Livneh et al., 2015). Within the suite of model inputs and outputs (see full list at: https://vic.readthedocs.io/en/master/Documentation/Drivers/Classic/ClassicDriver/), we focused on station-derived precipitation and simulated SWE, ET and PET. Snowmelt was computed as the negative change in SWE and SWI was the summation of snowmelt and rainfall at each time stamp (daily). VIC considers blowing snow sublimation within its snow model but no lateral transport of wind-blown snow across grid cells (Bowling et al., 2004). As previously stated in Hale et al. (2023), we assumed that negative changes in SWE were primarily associated with a melt flux, via a latent heat flux, as opposed to sublimation, given the order-of-magnitude difference between the latent heat of fusion and sublimation of water (Barnhart et al., 2016; Hood et al., 1999).

The VIC model has shown similarities in environmental conditions and outputs with other land surface models (Chen et al., 2015; Feng et al., 2008) when previously used to simulate the mountain snowpack (Elsner et al., 2010; Hamlet & Huppert, 2002; Hamlet & Lettenmaier, 1999; Mote et al., 2005; Vano & Lettenmaier, 2012; Vano et al., 2015). Similarly, the VIC-generated land surface and hydrologic flux variables have provided hydrologic estimates consistent with observations (Andreadis et al., 2009; Mote et al., 2018). Masked to the domain of interest, this study used data from the VIC version and parameterization of Livneh et al. (2015), which was validated against streamflow observations for the major river basins of CONUS. The Livneh et al. (2015) VIC simulation included a full iterative energy balance option and no explicit frozen soil option to ensure a conservative estimate of spring runoff magnitude and rate. It is acknowledged that overestimating frozen soils could overstate linkages between snowmelt and streamflow, while a conservative estimate could underestimate streamflow in some regions. The VIC model employs a rain–snow temperature range centered around a default of 50% rain–snow temperature threshold value, which was 0.0°C (Livneh et al., 2015). It is encouraged that future work explore additional model-based rain-snow air temperature and relative humidity thresholds to evaluate associated sensitivities around snowfall fraction and snowmelt (Jennings et al., 2018).

Precipitation and VIC-generated SWE data from this data set were used to generate long-term and annual snow water storage metrics (see Section 2.3), which were previously compared to ground-based snow observations generated from the automated SNOwpack TELemetry (SNOTEL) network in the western U.S. in Hale et al. (2023) for validation. Finally, VIC-generated ET and PET were compared against the Catchment Attributes and Meteorology for Large-Sample Studies (CAMELS) data set. This data set contains the daily variables needed to quantify additional annual snow water storage values using observational inputs (e.g., precipitation and temperature). Specifically, the CAMELS data set uses North American Land Data Assimilation System (NLDAS) precipitation inputs to optimize the Snow17 model against United States Geological Survey (USGS) streamflow gage sites to generate SWE outputs (Newman et al., 2015). Analyses have been completed to compare the modeled streamflow to observational stream gage data (Newman et al., 2015) and compare the corresponding SWE product to SNOTEL sites and additional snowpack models across CONUS and the western U.S. specifically (Duan et al., 2023; Raleigh & Lundquist, 2012). Future in-depth analyses on the timing of peak SWE and snowmelt are encouraged, since uncertainty exists across datasets yet accurately representing SWE greatly influences estimates of snow water storage (see Section 2.3). Finally, observed streamflow and modeled ET and PET data were also available within the CAMELS data set, which were needed to calculate (and compare) annual hydrologic partitioning, from 1980 to 2014 across the western U.S. (Newman et al., 2015).

2.3. The Snow Storage Index

The SSI was previously developed to represent the differences in temporal alignment (i.e., phase) and amplitude (i.e., magnitude) between precipitation seasonality and surface water inputs seasonality, creating a dimensionless value between −1 and 1 (Hale et al., 2023). This metric is wholly defined with further exemplar applications in Hale et al. (2023), and uses the methodology outlined in Woods (2009), generating, first, a precipitation sine curve, subscript P:

$$P(t) = \overline{P}\left[1 + \delta_P \sin\left(\frac{2\pi(t - s_P)}{365}\right)\right] \tag{1}$$

where $\overline{P}$ is the mean precipitation, t is the timestamp (days), s_P is the precipitation phase shift (days), and δ_P is a dimensionless seasonal amplitude of precipitation. s_P and δ_P are determined by fitting a nonlinear model to the daily precipitation data. Second, a SWI sine curve was developed:

$$\mathrm{SWI}(t) = \overline{\mathrm{SWI}}\left[1 + \delta_{\mathrm{SWI}} \sin\left(\frac{2\pi(t - s_{\mathrm{SWI}})}{365}\right)\right] \tag{2}$$

where $\overline{\mathrm{SWI}}$ is the mean SWI, (s_{SWI}) is the SWI phase shift (days), and δ_{SWI} is a dimensionless seasonal amplitude of SWI. s_{SWI} and δ_{SWI} are determined by fitting a nonlinear model to the daily SWI data. Finally, to generate the SSI, the two sine curves were combined, to compare the phase and amplitude of the SWI and P sine curves:

$$\mathrm{SSI} = -\left[\delta_{\mathrm{SWI}} \mathrm{sgn}(\delta_P) \cos\left(\frac{2\pi(s_{\mathrm{SWI}} - s_P)}{365}\right)\right] \tag{3}$$

Sgn represents the "sign" function, which extracts the sign of a real number. The final calculations were multiplied by −1 so that positive values corresponded with greater snow water storage. Thus, the differences between the phase (or timing) and the amplitude (or magnitude) of precipitation seasonality and SWI seasonality were evaluated, creating a dimensionless value between −1 (P and SWI in-phase with greater seasonality) and 1 (P and SWI out-of-phase with greater seasonality). We used annual average SSI values greater than 0 (the threshold where P and SWI have no seasonality) to focus on areas where there exists annual misalignment between falling P and SWI generation. The annual average SSI was used to explore the inter-annual surface water storage dynamics within each grid-cell. In addition to the SSI examples shown and outlined in Hale et al. (2023), relevant depictions of this methodology applied to daily precipitation and surface water inputs data across climates and mountain ranges are shown in Supporting Information S1 (Figure S1).

2.4. Ratios of Surface Water Inputs and Precipitation (SWI:P)

The ratio of weekly SWI to weekly precipitation (P) represents a proxy for snowpack water storage and release behavior, that is utilized in this research to complement the SSI-based analyses. We used a weekly and 30-day moving average of SWI:P as an additional independent environmental variable to compare against the dependent hydrologic partitioning metric (see Section 2.5). Because the SSI is a function of precipitation and SWI, the SWI:P ratio provides first-principle insights into daily to weekly snow water storage in a given region. If the SWI:P ratio is high (>1), more SWI occurred than P in a given time period, and the snowpack released stored water as snowmelt. If the SWI:P ratio is low (<1), more P occurred than SWI, and some P fell as snow and was stored in the snowpack. If the SWI:P ratio = 1, P either fell as rain or melted soon after falling as snow. Typically, areas with greater annual SSI values had a smaller SWI:P in winter/spring months and a larger SWI:P in late spring/summer months. Areas with lower annual SSI values experience a larger SWI:P in winter/spring months and a smaller SWI:P in late spring/summer months. Thus, this metric might be expected to closely relate to hydrologic partitioning, as weekly and 30-day moving averages of SWI:P capture the timing (and relative amount) of snow water storage for every week or day of the year. Examples of daily SWI:P ratios are also shown in Supporting Information S1 (Figure S1).

2.5. The Budyko Framework

A similar approach to Barnhart et al. (2016) and Berghuijs et al. (2014) was applied to quantify hydrologic partitioning using the VIC and CAMELS data and the Budyko framework (Budyko, 1974). Hydrologic partitioning, in this context, is defined as the annual fraction of precipitation (P) that becomes ET or streamflow (Q). Based on the climate conditions (i.e., aridity index), the Budyko framework was used to predict the amount of annual precipitation that would become streamflow or ET (Figure 1, black line). Anomalies from the Budyko hypothesis expectation, indicate over- or under-production of streamflow, where a positive anomaly indicates overproduction of streamflow from the expectation (Figure 1, blue point and bracket) and a negative anomaly indicates underproduction of streamflow, or overproduction of ET (Figure 1, yellow point and bracket). Thus, the use of the Budyko framework allows for a spatially and temporally distributed evaluation of long-term hydrologic partitioning behavior across the study domain.

Specifically, the expected partitioning behavior estimated from the Budyko framework was obtained for each VIC grid-cell and CAMELS watershed, relating the long-term aridity index (i.e., $\frac{PET}{P}$) to the long-term evaporative fraction (i.e., $\frac{ET}{P}$):

$$\frac{ET_{expected}}{P_{expected}} = \sqrt{\left(\frac{PET}{P}\tanh\left(\frac{P}{PET}\right)\right)\left(1-\exp\left(-\frac{PET}{P}\right)\right)} \tag{4}$$

The Budyko framework thus served as the expected $\frac{ET}{P}$ (or $1-\frac{Q}{P}$) for any $\frac{PET}{P}$ value (Figure 1, black line). An anomaly from the expectation indicated over or underproduction of ET or Q relative to the expectation (Figure 1 blue and yellow points and brackets):

$$\frac{ET_{anom}}{P} = \frac{ET_{expected}}{P_{expected}} - \frac{ET_{VIC}}{P_{VIC}} \tag{5}$$

where $\frac{ET_{anom}}{P}$ is the vertical difference between the expected $\frac{ET}{P}$, per the Budyko hypothesis, and the $\frac{ET}{P}$ fraction from the VIC or CAMELS data sets. We subsequently evaluated potential relationships between annual average SSI and SWI:P ratios and the Budyko anomaly ($\frac{ET_{anom}}{P}$). We evaluated deviations of each VIC grid-cell and CAMELS lumped watersheds from expected hydrologic partitioning, and then grouped grid-cells and watersheds

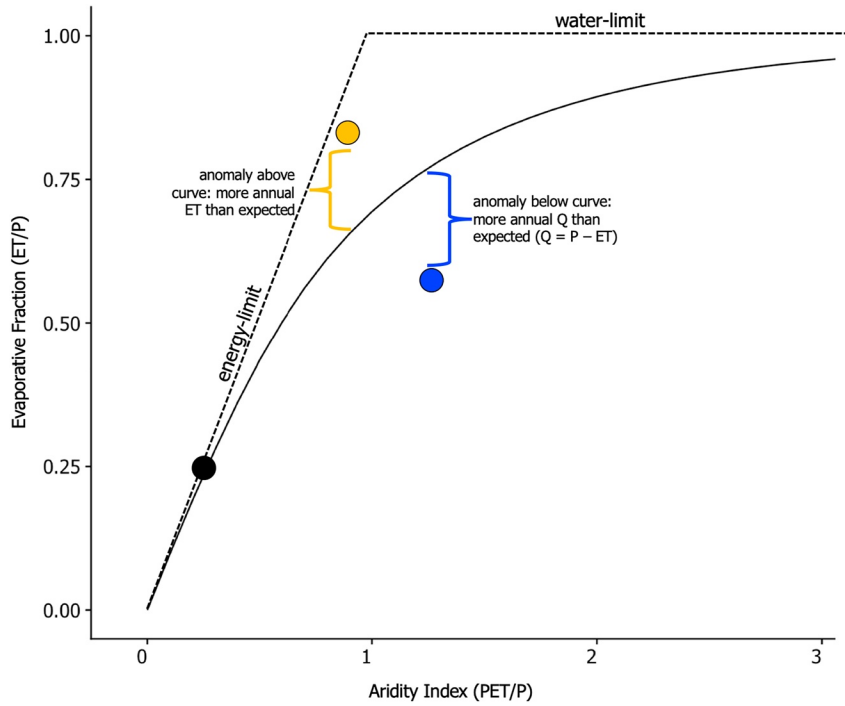

Figure 1. Hypothetical depiction of the Budyko framework (Budyko, 1974), used to predict the amount of annual precipitation (P) which will become evaporated (evapotranspiration (ET)) or streamflow (Q), based on an index of the catchment aridity (potential evapotranspiration (PET)/P). The black line represents the Budyko expectation. Energy-limited catchments are classified as PET/P < 1, and water-limited catchments are classified as PET/P > 1. The black point represents a catchment which partitions annual water inputs as expected. The yellow point represents a catchment which partitions more water inputs to ET than expected, and the yellow bracket is the quantifiable anomaly from the Budyko hypothesis. Finally, the blue point represents a catchment which partitions more water inputs to Q than expected, and the blue bracket is the anomaly from the expectation. To quantify anomalous behavior, the vertical difference between the line and the point is taken. Thus, positive anomaly values indicate points falling below the line, and negative anomaly values indicate points falling above the line.

across eco-regions. Deviations from expected partitioning values, evaluated relative to the SSI, were used to infer how water storage within snowpacks influenced hydrologic partitioning behavior, and to infer the climate sensitivity of hydrologic behavior.

To secondarily explore differences in hydrologic partitioning associated to climate, the long-term average precipitation, temperature, and aridity index were used to differentiate between arid and humid eco-regions. Energy limitations generally existed when $\frac{\mathrm{PET}}{P} < 1$, and water limitations existed when $\frac{PET}{P} > 1$, (shown in Figure 1). These limitations guided the grouping of mountainous eco-regions across the western U.S.

3. Results

Twenty-six percent the study area had an annual average SSI greater than 0 (Figure 2a, $n = 7{,}173$ of 27,560 total grid-cells in the western cordillera), signifying the areas in which snowpack water storage acts to decouple the timing of P and SWI generation. Extensive areas of high annual SSI values (>0.75) existed in the eco-regions of the North Cascades, Cascades, Columbia Mountains/Northern Rockies, Idaho Batholith and Middle Rockies (labeled in Figure 2a). Mid-range annual SSI values (0.5–0.75) existed in the Sierra Nevada, Wasatch and Uinta Mountains, and Southern Rockies. Spatial similarities in annual average SSI were reflected in the station-based CAMELS data set (Figure 2b, $n = 62$ stations), where greater annual average SSI values were seen in northern eco-regions and the central part of the Middle and Southern Rockies.

All VIC grid-cells fell within the physical limits of Budyko space (Figure 3, colored by SSI). Each eco-region showed a slightly different relationship between the annual average SSI and the Budyko anomaly (Figure 4, both r^2 and R_s $p \leq 0.05$ in all eco-regions). Yet, in almost all instances, the significant relationship between SSI and the

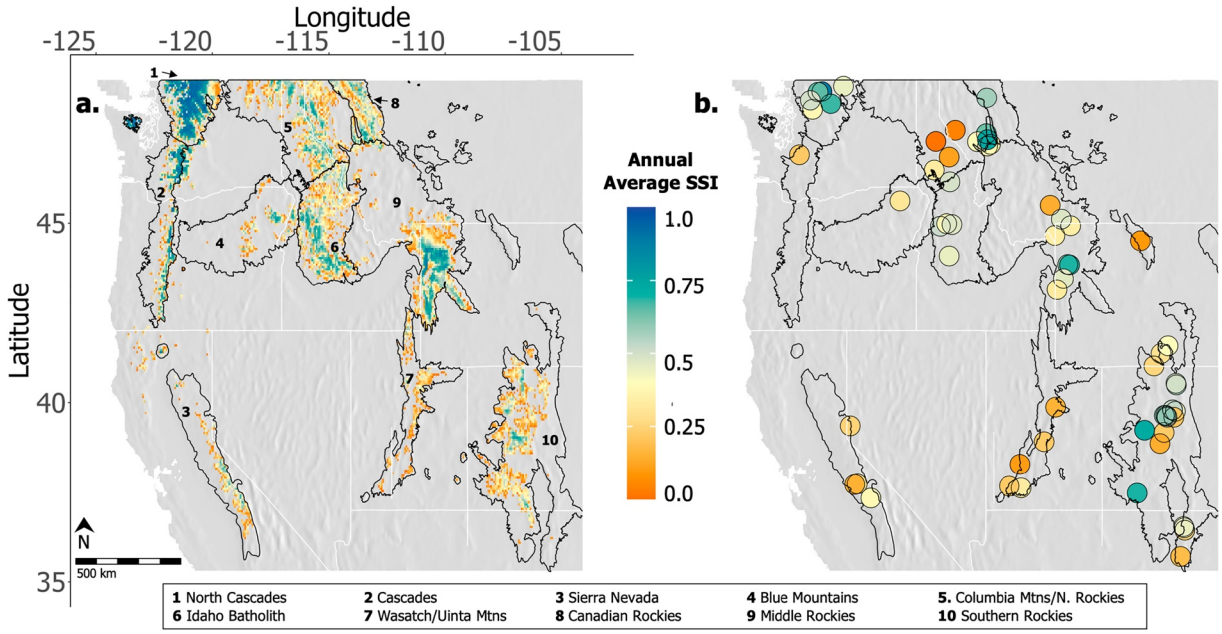

Figure 2. Annual average Snow Storage Index (SSI), where annual average SSI ≥ 0, across the (a) 64-year Variable Infiltration Capacity model output record (n = 7,173), and, (b) 34-year Catchment Attributes and Meteorology for Large-Sample Studies data set record (n = 62). Maritime eco-regions and climates exist in North Cascades, Cascades, and Sierra Nevada; and inter-mountain/continental eco-regions and climates exist in Blue Mountains, Idaho Batholith, Canadian Rockies, Columbia Mountains/Northern Rockies, Middle Rockies, Wasatch/Uinta Mountains, Southern Rockies.

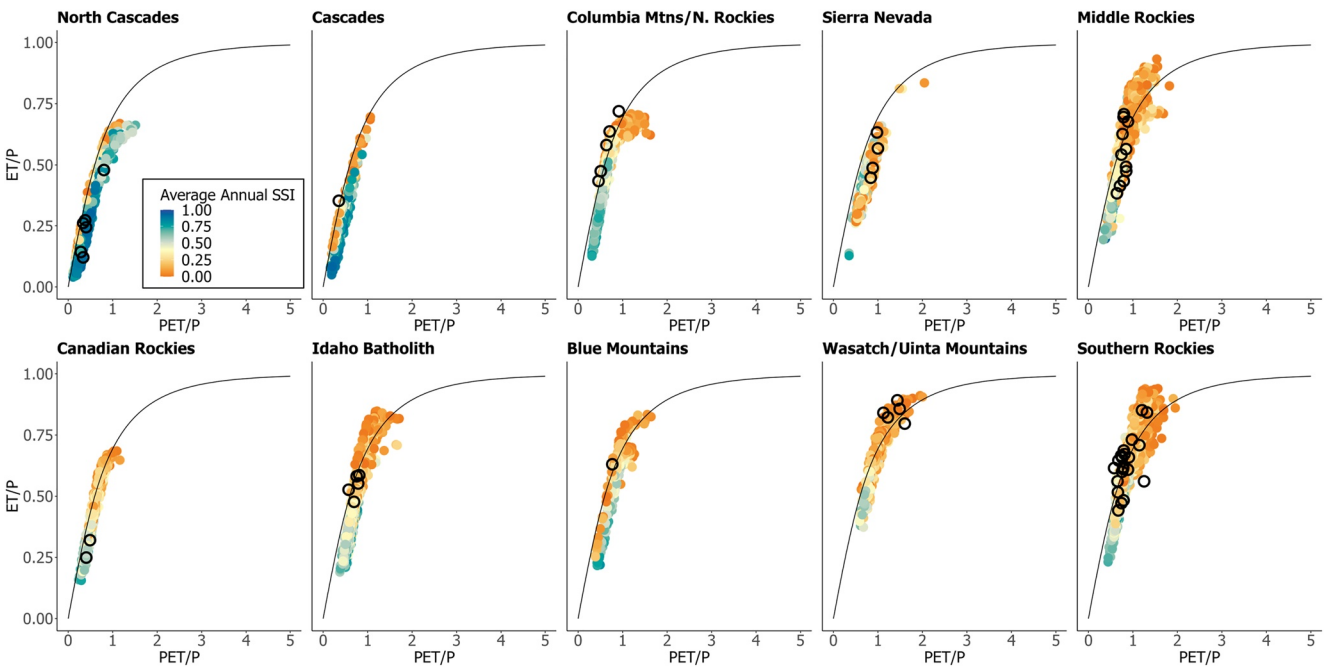

Figure 3. Long-term average aridity ($\frac{PET}{P}$) and evaporative ($\frac{ET}{P}$) fractions within Budyko space (Budyko, 1974) for 10 mountainous eco-regions across the western United States. The eco-regions classified as energy-limited are the six left-most panels, and the eco-regions classified as water-limited are the four right-most panels. Variable Infiltration Capacity grid cells are colored by average annual Snow Storage Index. Black open circles indicate the Catchment Attributes and Meteorology for Large-Sample Studies data within each eco-region.

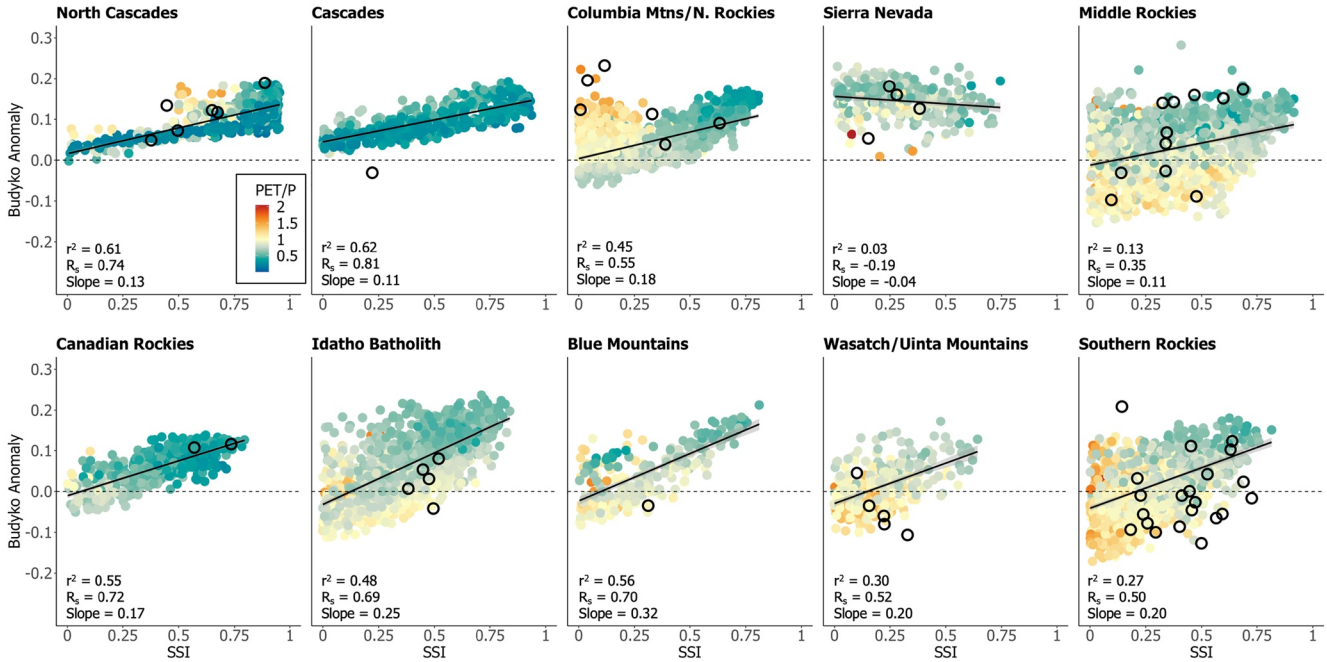

Figure 4. Annual average Snow Storage Index compared to the Budyko anomaly per grid-cell, per eco-region across the western United States. All relationships are statistically significant (linear and Spearman rank $p < 0.05$). Shading represents the 95% confidence interval, and Variable Infiltration Capacity grid cells are colored by average annual aridity ($\frac{PET}{P}$). Corresponding slope, linear r^2 values and Spearman rank correlation values (R_s) are listed in each panel. Positive Budyko anomalies indicate overproduction of streamflow, whereas negative Budyko anomalies indicate underproduction of streamflow. Black open circles indicate the Catchment Attributes and Meteorology for Large-Sample Studies data within each eco-region.

Budyko anomaly was positive in slope, with greater SSI values associated with a greater Budyko anomaly (i.e., more streamflow production than expected). While this relationship was generally linear, we reported both r^2 values and Spearman rank correlation values (R_s) to account for potential non-linear relationships. The relationship between the SSI and the Budyko anomaly was positive in slope and strongest in the Cascades ($r^2 = 0.62$, $R_s = 0.81$), North Cascades ($r^2 = 0.61$, $R_s = 0.74$), Blue Mountains ($r^2 = 0.56$, $R_s = 0.70$), Canadian Rockies ($r^2 = 0.55$, $R_s = 0.72$), Idaho Batholith ($r^2 = 0.48$, $R_s = 0.69$), and Columbia Mountains/Northern Rockies ($r^2 = 0.45$, $R_s = 0.55$).

The relationship between annual average SSI and the Budyko anomaly was relatively weak and positive in slope in the Middle Rockies ($r^2 = 0.13$, $R_s = 0.35$), Wasatch and Uinta Mountains ($r^2 = 0.30$, $R_s = 0.52$) and Southern Rockies ($r^2 = 0.20$, $R_s = 0.50$). The SSI-Budyko anomaly relationship was weak and negative in slope in the Sierra Nevada ($r^2 = 0.03$, $R_s = -0.19$). On average across the western U.S., areas with greater annual average SSI values partitioned a larger proportion of annual precipitation to streamflow relative to the expected proportion from the Budyko hypothesis ($r^2 = 0.29$, $p \leq 0.05$, not shown). Thus, larger SSI values result in a larger Budyko anomaly, as areas storing more water in the snowpack for a longer period of time were more efficient at partitioning precipitation to streamflow than areas with a smaller SSI value.

Across the four defined and distinct eco-region groups, separated by climate and relative water versus energy limitations (Figure 5a), the relationship between annual average SSI and the Budyko anomaly was particularly strong and positive in slope in more energy-limited eco-regions, in both maritime ($r^2 = 0.57$) and inter-mountain/continental ($r^2 = 0.42$) climates (Figures 5b and 5c). The relationship was significant ($p \leq 0.05$) but weak ($r^2 = 0.03$) and negative in slope in water-limited, maritime eco-regions; and relatively weak ($r^2 = 0.20$) and positive in slope in inter-mountain/continental eco-regions (Figures 5d and 5e). The CAMELS data fell within the spread of VIC grid-cells within the four groups of eco-regions (Figures 5a–5e).

Weekly SWI:P ratios were strongly related to hydrologic partitioning to streamflow, primarily in more energy-limited eco-regions and during periods of relatively high snowpack water storage. For example, Figure 6 shows the weekly SWI:P-Budyko anomaly relationship in the North Cascades from early March to mid-August, where all weeks showed significance ($p < 0.05$) except the week of May 20. In spring months, smaller volumes of weekly SWI were produced in areas within the North Cascades eco-region that had a larger SSI value (>0.75).

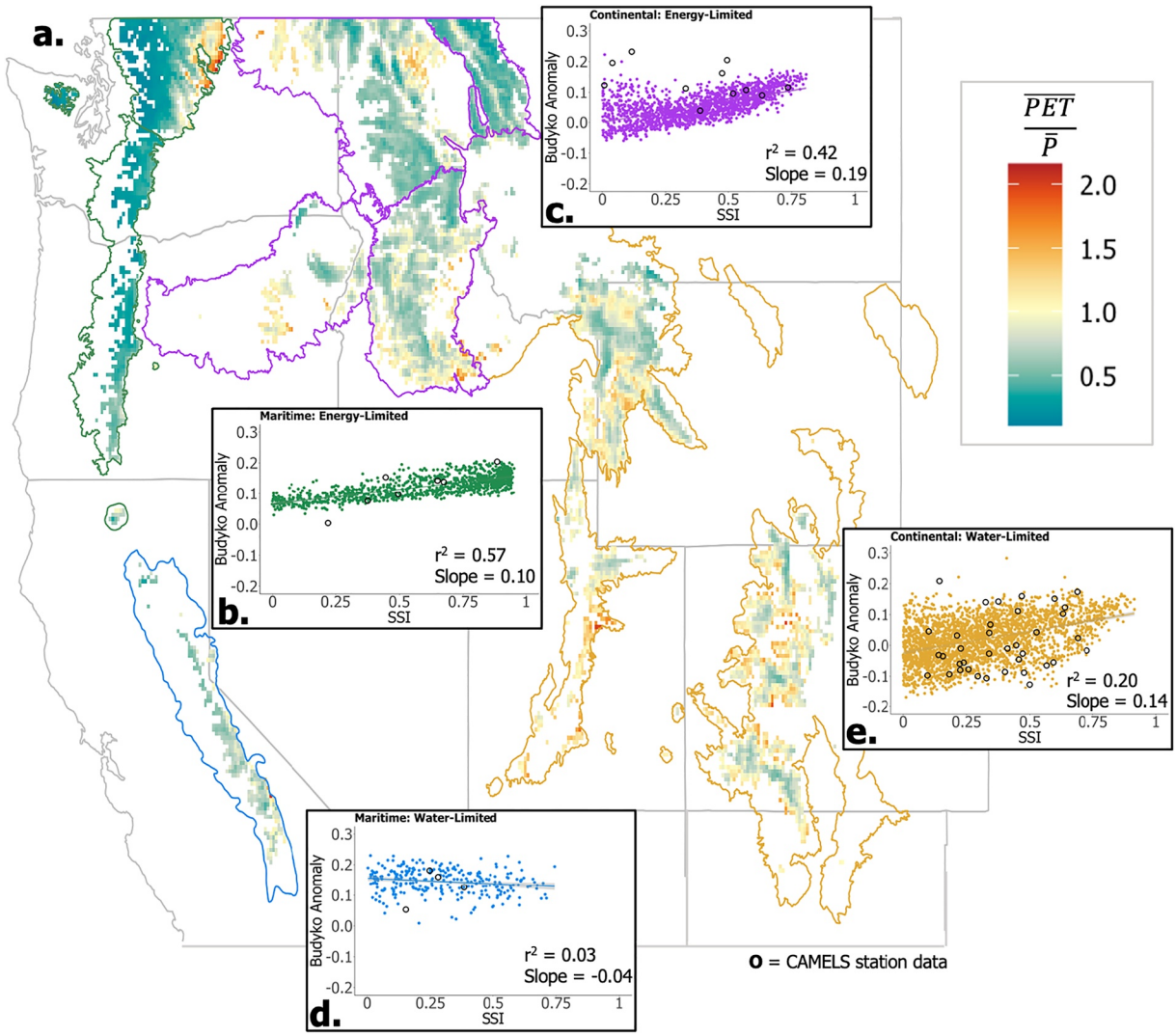

Figure 5. (a) Long-term aridity index ($\frac{PET}{P}$) across the domain, guiding the generation of four eco-region groups, outlined in four distinct colors; where the average annual Snow Storage Index was then compared to the Budyko anomaly per grid cell, across the bins of data: (b) (green) Maritime, more energy-limited eco-regions; (c) (purple) Continental, more energy-limited eco-regions; (e) (blue) Maritime, more water-limited eco-regions, and; (e) (yellow) Continental, more water-limited eco-regions. All relationships are statistically significant ($p < 0.05$), and associated r^2 and slope values are listed on each panel. Black open circles indicate the Catchment Attributes and Meteorology for Large-Sample Studies data within each eco-region.

Comparatively, areas within the North Cascades with smaller SSI values (<0.5) had produced large SWI volumes in spring. Areas within the eco-region with a smaller weekly SWI:P ratio in March/April (i.e., greater SSI) produced a larger annual Budyko anomaly, compared to areas within the eco-region with a larger SWI:P ratio (i.e., lower SSI) during these spring weeks, which consistently produced a smaller Budyko anomaly (Figure 6, top row). This resulted in a strong relationship (max $r^2 = 0.74$), negative in slope, between weekly spring SWI:P ratios and the Budyko anomaly. Thus, low spring SWI:P ratios resulted in greater partitioning to streamflow in the North Cascades.

The slope of the weekly SWI:P-Budyko anomaly relationship decreased in magnitude during the months of May and early June (Figure 6, second and third rows), until the weekly SWI:P-Budyko anomaly slope became positive in late June and July (Figure 6, bottom row). More SWI was produced during June/July in areas of the North Cascades with a larger SSI value, and less SWI was produced in areas with a smaller SSI value. In turn, areas with a larger SWI:P ratio (large SSI) in June/July produced a larger Budyko anomaly, and areas with a smaller SWI:P ratio (smaller SSI) produced a smaller Budyko anomaly. Thus, larger summer SWI:P ratios, associated with the release of water storage from the snowpack, resulted in more partitioning to streamflow.

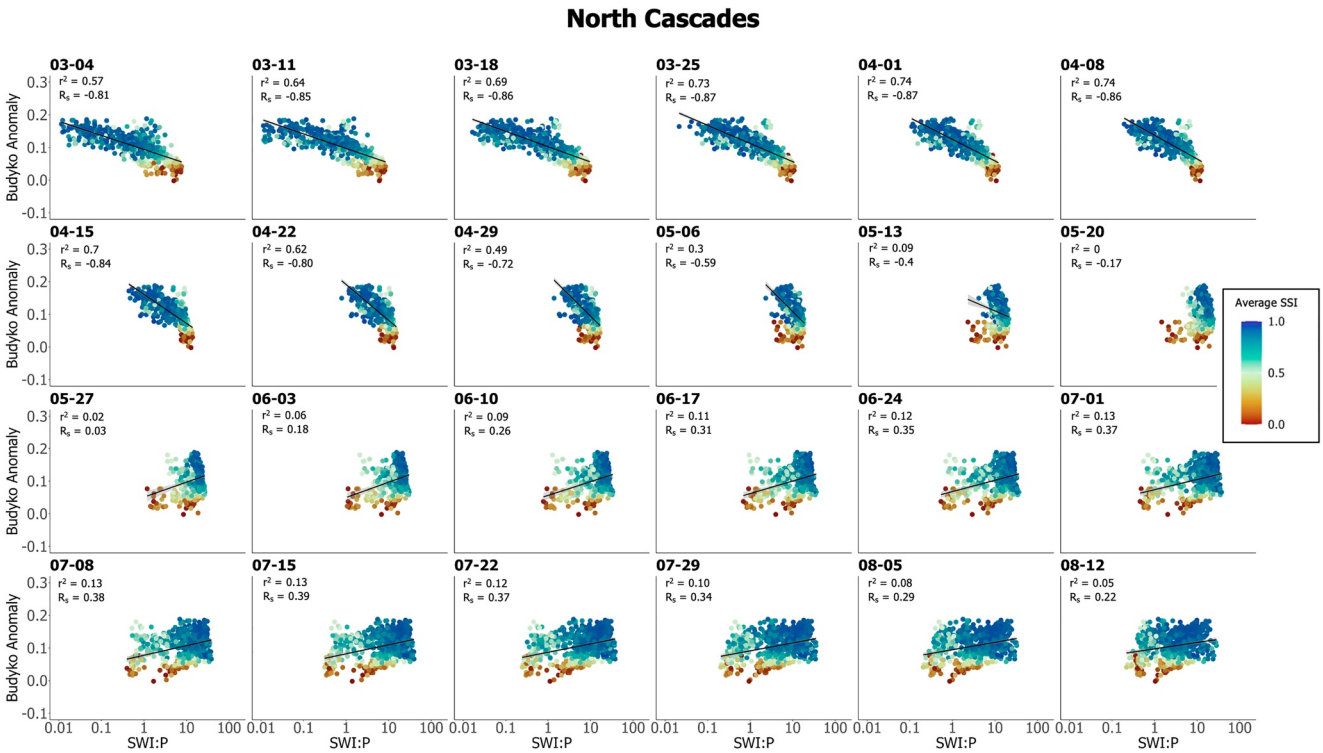

Figure 6. Weekly SWI:P in the North Cascades, exemplar of an energy-limited eco-region. Greater Snow Storage Index (SSI) grid-cells store water in the snowpack in spring months (April/May), and thus SWI:P is small, compared to lower SSI regions which release snowmelt from the snowpack earlier in the year (top row). Trend lines have been added to panels where the relationship between SWI:P and the Budyko anomaly is significant (linear and Spearman rank $p < 0.05$). *X*-axes are logarithmic, and corresponding linear r^2 values and Spearman rank correlation values (R_s) are included.

Consistent across all energy-limited eco-regions, the relationships between the weekly SWI:P ratio and the Budyko anomaly were strongest in the spring months (maximum $r^2 = 0.62$–0.74, not shown for all eco-regions). These relationships were also assessed using logarithmic and exponential functions, however, the difference between linear and non-linear r^2 values were never more than 5% or 2%, respectively. In turn, we have reported just the linear r^2 value and Spearman rank correlation value (R_s) (e.g., Figures 6 and 7 on a logarithmic scale). The analysis was also conducted using a 30-day moving window to explore constraints around organizing by calendar weeks, but we found that, ultimately, evaluating these variables weekly was suitable in providing a first principle explanation for SWI:P controls on the Budyko anomalies.

The dynamic relationship between weekly SWI:P ratios and the Budyko anomaly was less prominent in relatively water-limited eco-regions (across both maritime and inter-mountain/continental climates). Figure 7 shows the Southern Rockies as a contrasting example to the North Cascades example shown in Figure 6. Through the same 5-month period, little partitioning sensitivity to weekly SWI:P ratios existed. The relationships were significant during the weeks of 4 March, 18 March, 1 April–22 April, 6 May–12 August. The slope of the relationships between weekly SWI:P and the Budyko anomaly were similar in sign as seen in the North Cascades; that is, there was a negative slope in spring months, transitioning to positive slope in summer months. However, the strength of the relationships was relatively weak in comparison (maximum $r^2 < 0.3$). The relatively weak relationships, in addition to those seen in Figures 4 and 5, suggest that the sensitivity of hydrologic partitioning to variability in snow water storage was relatively modest in more water-limited eco-regions compared to the strong explanatory signal seen in more energy-limited eco-regions.

4. Discussion

On average, regions with greater SSI values partitioned more annual precipitation volume to streamflow than what would be expected based on the Budyko hypothesis (Figure 4). This relationship was especially prominent in more energy-limited eco-regions (Figures 4, 5b, and 5c). These same regions exhibited distinct snow water storage and water release periods in the spring/summer months, and the associated weekly SWI:P

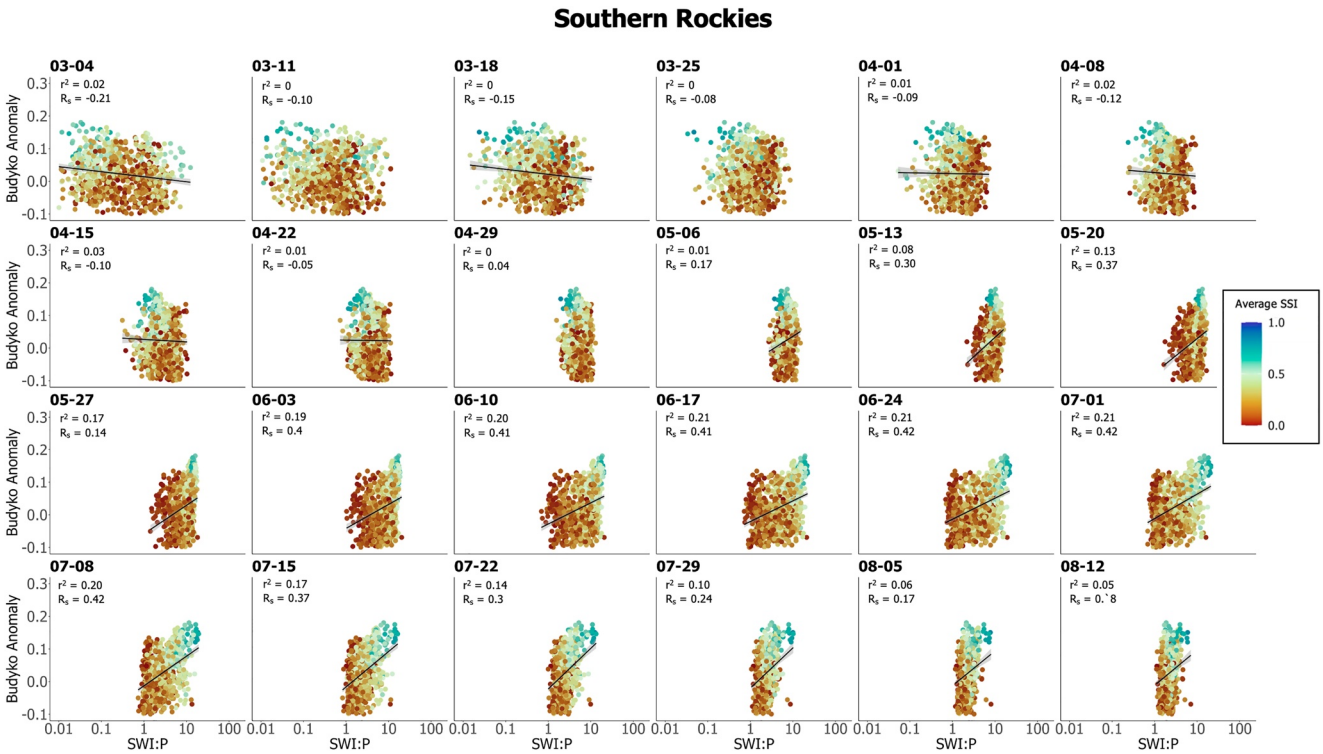

Figure 7. Weekly SWI:P in the Southern Rockies, exemplar of a continental, more water-limited eco-region. Trend lines have been added to panels where the relationship between SWI:P and the Budyko anomaly is significant (linear and Spearman rank $p < 0.05$). *X*-axes are logarithmic, and corresponding linear r^2 values and Spearman rank correlation values (R_s) are included.

ratios were strongly related to hydrologic partitioning (Figure 6). Thus, where water was stored in the snowpack throughout spring months (March/April) and released later in summer months (June/July), more annual precipitation ultimately became streamflow than expected. In addition to historic declines in snowfall and mean and peak SWE (Mote et al., 2018; Stewart, 2009; Stewart et al., 2004), regional snow water storage, as defined by the SSI, has also declined (revealed in Hale et al. (2023)), which indicates that hydrologic partitioning to streamflow may also decline, partitioning less water to streamflow and decreasing the amount of available downstream water.

Referring to the introduction of this work, in which two opposing hypotheses were presented in the context of hydrologic partitioning sensitivities to snow water storage, the results of this work indeed confirm that the first hypothesis (i.e., the role of snow water storage in generating a large and fast late-spring/summer snowmelt pulse) seems to dominate the hydrology in more energy-limited eco-regions (Figure 6) (Barnhart et al., 2016). The second hypothesis (i.e., the role of snow water storage in aligning SWE and PET) may be counter-acting the first hypothesis in a rather significant manner in more water-limited areas (Figure 7) (Foster et al., 2016; Jeton et al., 1996). The strength of the SSI- and SWI:P-Budyko anomaly relationships in energy-limited eco-regions also suggests that these catchments are more sensitive to changes in snow water storage than water-limited eco-regions, as it pertains to hydrologic partitioning. These energy-limited eco-regions have also shown to be the areas of highest sensitivity to changes in temperature and thus snowpack (Mote et al., 2018).

The relationship between the snow water storage metric (SSI) and hydrologic partitioning ultimately provides a physical rationale for the partitioning relationships seen in past works, which highlight snow fraction and snowmelt rate as controlling variables of hydrologic partitioning (Barnhart et al., 2016; Berghuijs et al., 2014). The results seen here, relating expected versus observed or modeled streamflow to both the SSI (i.e., $r^2 = 0.45$–0.62 across eco-regions) and SWI:P ratios (Figures 6 and 7) are significantly stronger than the relationship between snow fraction and Budyko anomalies illustrated in Berghuijs et al. (2014) (i.e., $r^2 = 0.3$, $n = 420$) or within our study ($r^2 = 0.18$, $n = 7{,}173$, not shown). This is because a high snow fraction does not necessarily indicate greater snow water storage. Instead, the uniqueness of the SSI is to additionally capture the temporal component between snowfall and snowmelt, as well as the magnitude of both. Snowmelt rates show comparable control on water partitioning

(Barnhart et al., 2016), particularly because the rate of snowmelt is dependent on energy availability, which varies seasonally (Musselman et al., 2017). Thus, a uniting explanatory variable, providing a first principle mechanism for annual hydrologic partitioning, is snow water storage and the degree to which various regions store and release water, in volume and in time.

Importantly, the SSI is a metric that captures differences in timing and magnitude of precipitation and surface water inputs beyond solely SWE residence time or SWE magnitude. Whereas SWE residence time may be long in high, cold environments like the Southern Rockies (Harpold et al., 2012), nuances to the SSI exist where summer rainfall acts to reduce seasonality in precipitation and SWI and thus decrease the SSI. As a result, decreases or increases in annual partitioning of water to streamflow may occur, depending on the climate and elevation (Carroll et al., 2020). These nuances are not otherwise captured in current metrics used as proxies for water availability, such as average or peak SWE, adding analytical power to the SSI. The SSI further complements existing indices developed for evaluating the integrative hydrologic impact of seasonal snow, such as the temporal lag between precipitation and snowmelt used to identify downstream hydrologic deficits from snowmelt and rainfall (Staudinger et al., 2014) and the potential for snowmelt to meet downstream demands in hydrologically vulnerable regions of the world (Hale et al., 2023; Immerzeel et al., 2020; Mankin et al., 2015).

The model-derived SSI data were compared to observational SSI data, derived from SNOTEL station data, in the western U.S. in Hale et al. (2023) (r^2 = 0.51) and compared to additional SSI data, derived from the CAMELS data set, here (Newman et al., 2015). SSI differences between VIC grid-cells (6 km scale) and observation-based CAMELS lumped watersheds may exist due to the differing spatial scales (Livneh & Badger, 2020; Newman et al., 2015), record lengths, and corresponding snow models in use (Andreadis et al., 2009; Newman et al., 2015). A higher spatial model resolution would need to be investigated in future work to more thoroughly explore snow water storage and partitioning relationships and the error associated with spatial scale. The VIC model physics likely affect the relationship between SSI and the Budyko anomaly seen within the model data, via its baseflow parameterization (e.g., nonlinear or linear). For example, if employing a nonlinear baseflow parameterization, the model will be more efficient at generating runoff when soil moisture storage in the third layer is above a given threshold, which could occur more frequently in the energy-limited areas (Bao et al., 2012). VIC also computes deep percolation loss to ground water, which may influence annual partitioning (Bowling et al., 2004; Liang et al., 1994). Future efforts should consider the effects of the subsurface and relevant connectivity among soil, groundwater, and vegetation (Cayan et al., 2010; McNamara et al., 2005). Future work should also include recent advances in the rain-snow phase partitioning temperature threshold (set as 0.0°C in this model version) (Jennings & Molotch, 2019). The effect of the rainfall/snowfall temperature threshold could be particularly important in more arid regions, where this threshold is often above 0.0°C (Jennings & Molotch, 2019) and where the quality of the estimated air temperatures in VIC is potentially lower (Livneh et al., 2015).

Climate warming has caused fundamental changes to the hydrologic cycle in the mountainous west with remaining unknown effects on the sensitivities of water availability (Berghuijs et al., 2014; Foster et al., 2016; Gupta & Soroosh, 1998; Hinckley et al., 2012; Livneh & Badger, 2020; Safeeq et al., 2013). In recent decades, runoff sensitivities to high temperatures have become exacerbated, particularly in semi-arid, water-limited regions, where snowmelt is a primary water source (Lehner et al., 2017). This work addresses an important knowledge gap in mountain hydrology by assessing the mechanisms by which snow water storage impacts hydrologic partitioning (Berghuijs et al., 2014; Bosson et al., 2012; Groisman et al., 2004; Mote et al., 2005, 2018). Regional snow fraction, snowmelt rate and SWE trend analyses do not alone capture the timing of water availability to terrestrial systems (Barnhart et al., 2016; Berghuijs et al., 2014; Mote et al., 2005, 2018; Zhang et al., 2015). These previously studied variables, while important, do not explicitly represent the role of snowpack water storage in the hydrologic cycle or catchment water balance. The SSI is unique in that it quantifies the timing and relative magnitude of water availability in these regions. In turn, the SSI and SWI:P ratios provide a metric to assess spatial differences in hydrologic partitioning, by way of the Budyko hypothesis framework. Hale et al. (2023) showed that average snow water storage across western North America is decreasing. As snow water storage continues to decline in response to warming, a shift in seasonal SWI:P ratio is expected. Consequently, decreased snow water storage, particularly in energy-limited catchments, may cause a decrease in hydrologic partitioning to streamflow, placing a strain on downstream water availability, which may exacerbate other mechanisms leading to shortages in regional water supplies (Griffin & Anchukaitis, 2014; Immerzeel et al., 2020).

5. Conclusion

A snow water storage metric (SSI) and weekly surface water inputs-precipitation (SWI:P) ratios were directly related to hydrologic partitioning, by way of the Budyko framework. The SSI was positively correlated with greater hydrologic partitioning to streamflow than expected, particularly in the Cascades (r^2: 0.62), North Cascades (r^2: 0.61), Blue Mountains (r^2: 0.56), Canadian Rockies (r^2: 0.55), Idaho Batholith (r^2: 0.48), and Columbia Mountains/Northern Rockies (r^2: 0.45). These results indicate more streamflow partitioning associated with greater snow water storage. Similarly, these eco-regions showed strong relationships between streamflow production and seasons of water storage (e.g., March/April), represented by a ratio of SWI to precipitation (P), where greater early season water storage in the snowpack was related to increased annual hydrologic portioning to streamflow ($r^2 = 0.62$–0.74). The Sierra Nevada, Middle Rockies, Wasatch/Uinta Mountains, Southern Rockies showed less sensitivity of hydrologic partitioning to SSI and SWI:P ($r^2 < 0.3$). The relationships between SSI and SWI:P ratios, and the Budyko anomalies revealed herein provide mechanistic insights on hydrologic partitioning in snow water storing areas. The results fill an important knowledge gap by relating time-magnitude dimensions of snow water storage, by way of the SSI, to annual streamflow partitioning. Snow water storage across Earth's mountain ranges are highly sensitive to climate warming. As snow water storage declines, hydrologic partitioning to streamflow may also decline, with large implications for future water resources across the western U.S., with potential global implications.

Data Availability Statement

To access the formatted annual (1950–2013) VIC-modeled Snow Storage Index products, please visit: https://doi.org/10.5061/dryad.3bk3j9kpn. Meteorological data used to force the Variable Infiltration Capacity (VIC) model across North America from 1950 to 2013 were downloaded from the NOAA National Centers for Environmental Information (https://www.ncei.noaa.gov/access/metadata/landing-page/bin/iso?id=gov.noaa.nodc:Livneh-Model). The resulting flux data were downloaded from the same source. The semi-observational Catchment Attributes and Meteorology for Large-sample Studies (CAMELS) data set was downloaded from the National Center for Atmospheric Research (https://ral.ucar.edu/solutions/products/camels). Level III eco-region boundaries for mapping and analysis were accessed from the EPA (https://www.epa.gov/eco-research/level-iii-and-iv-ecoregions-continental-united-states).

Acknowledgments
This research has been supported by the National Aeronautics and Space Administration (NNX17AF50G, 80NSSC17K0071, 80NSSC20K1420), the National Oceanic and Atmospheric Administration (NA15OAR4310144), the Western Water Assessment (NA21OAR4310309), and by the National Center for Atmospheric Research, which is a major facility sponsored by the National Science Foundation (Cooperative Agreement No. 1852977).

References

Adam, J. C., Clark, E. A., Lettenmaier, D. P., & Wood, E. F. (2006). Correction of global precipitation products for orographic effects. *Journal of Climate*, *19*(1), 15–38. https://doi.org/10.1175/JCLI3604.1

Alonso-González, E., Revuelto, J., Fassnacht, S. R., & Lopez-Moreno, J. I. (2022). Combined influence of maximum accumulation and melt rates on the duration of the seasonal snowpack over temperate mountains. *Journal of Hydrology*, *608*, 127574. https://doi.org/10.1016/j.jhydrol.2022.127574

Andreadis, K. M., Storck, P., & Lettenmaier, D. P. (2009). Modeling snow accumulation and ablation processes in forested environments. *Water Resources Research*, *45*(5), W05429. https://doi.org/10.1029/2008wr007042

Anghileri, D., Voisin, N., Castelletti, A., Pianosi, F., Nijssen, B., & Lettenmaier, D. (2016). Value of long-term streamflow forecasts to reservoir operations for water supply in snow- dominated river catchments. *Water Resources Research*, *52*(6), 4209–4225. https://doi.org/10.1002/2015wr017864

Bao, Z., Zhang, J., Liu, J., Fu, G., Wang, G., He, R., et al. (2012). Comparison of regionalization approaches based on regression and similarity for predictions in ungauged catchments under multiple hydro-climatic conditions. *Journal of Hydrology*, *466*, 37–46. https://doi.org/10.1016/j.jhydrol.2012.07.048

Barnett, T. P., Adam, J. C., & Lettenmaier, D. P. (2005). Potential impacts of a warming climate on water availability in snow-dominated regions. *Nature*, *438*(7066), 303–309. https://doi.org/10.1038/nature04141

Barnhart, T. B., Molotch, N. P., Livneh, B., Harpold, A. A., Knowles, J. F., & Schneider, D. (2016). Snowmelt rate dictates streamflow. *Geophysical Research Letters*, *43*(15), 8006–8016. https://doi.org/10.1002/2016gl069690

Barnhart, T. B., Tague, C. L., & Molotch, N. P. (2020). The counteracting effects of snowmelt rate and timing on runoff. *Water Resources Research*, *56*(8), e2019WR026634. https://doi.org/10.1029/2019wr026634

Berghuijs, W., Woods, R., & Hrachowitz, M. (2014). A precipitation shift from snow towards rain leads to a decrease in streamflow. *Nature Climate Change*, *4*(7), 583–586. https://doi.org/10.1038/nclimate2246

Bosson, E., Sabel, U., Gustafsson, L. G., Sassner, M., & Destouni, G. (2012). Influences of shifts in climate, landscape, and permafrost on terrestrial hydrology. *Journal of Geophysical Research*, *117*(D5), D05120. https://doi.org/10.1029/2011jd016429

Bowling, L. C., Pomeroy, J. W., & Lettenmaier, D. P. (2004). Parameterization of blowing snow sublimation in a macroscale hydrology model. *Journal of Hydrometeorology*, *5*(5), 745–762. https://doi.org/10.1175/1525-7541

Brooks, P. D., Chorover, J., Fan, Y., Godsey, S. E., Maxwell, R. M., McNamara, J. P., & Tague, C. (2015). Hydrological partitioning in the critical zone: Recent advances and opportunities for developing transferable understanding of water cycle dynamics. *Water Resources Research*, *51*(9), 6973–6987. https://doi.org/10.1002/2015wr017039

Brown, R. D., & Mote, P. W. (2009). The response of Northern Hemisphere snow cover to a changing climate. *Journal of Climate*, *22*(8), 2124–2145.
Brown, R. D., & Robinson, D. A. (2011). Northern Hemisphere spring snow cover variability and change over 1922–2010 including an assessment of uncertainty. *The Cryosphere*, *5*(1), 219–229.
Budyko, M. I. (1974). *Climate and life*. Academic Press.
Carroll, R. W., Gochis, D., & Williams, K. H. (2020). Efficiency of the summer monsoon in generating streamflow within a snow-dominated headwater basin of the Colorado River. *Geophysical Research Letters*, *47*(23), e2020GL090856. https://doi.org/10.1029/2020gl090856
Cayan, D. R., Das, T., Pierce, D. W., Barnett, T. P., Tyree, M., & Gershunov, A. (2010). Future dryness in the southwest US and the hydrology of the early 21st century drought. *Proceedings of the National Academy of Sciences of the United States of America*, *107*(50), 21271–21276. https://doi.org/10.1073/pnas.0912391107
Cayan, D. R., Kammerdiener, S. A., Dettinger, M. D., Caprio, J. M., & Peterson, D. H. (2001). Changes in the onset of spring in the western United States. *Bulletin of the American Meteorological Society*, *82*(3), 399–415. https://doi.org/10.1175/1520-0477(2001)082<0399:citoos>2.3.co;2
Chen, F., Barlage, M., Tewari, M., Rasmussen, R., Jin, J., Lettenmaier, D., et al. (2015). Modeling seasonal snowpack evolution in the complex terrain and forested Colorado Headwaters region: A model intercomparison study. *Journal of Geophysical Research: Atmospheres*, 1–25. https://doi.org/10.1002/(ISSN)2169-8996
Clow, D. W. (2010). Changes in the timing of snowmelt and streamflow in Colorado: A response to recent warming. *Journal of Climate*, *23*(9), 2293–2306. https://doi.org/10.1175/2009JCLI2951.1
Commission for Environmental Cooperation. (2011). *Ecological regions of North America, Level 3, scale 1:4,000,000*. Commission for Environmental Cooperation.
Conway, J., Carey-Smith, T., Cattoën-Gilbert, C., Moore, S., Sirguey, P., & Zammit, C. (2021). Simulations of seasonal snowpack duration and water storage across New Zealand. *Weather and Climate*, *41*(1), 72–89. https://doi.org/10.2307/27127990
Duan, S., Ullrich, P., Risser, M., & Rhoades, A. (2023). Using temporal deep learning models to estimate daily snow water equivalent over the Rocky Mountains. *Authorea Preprints*.
Elias, E., James, D., Heimel, S., Steele, C., Steltzer, H., & Dott, C. (2021). Implications of observed changes in high mountain snow water storage, snowmelt timing and melt window. *Journal of Hydrology: Regional Studies*, *35*, 100799. https://doi.org/10.1016/j.ejrh.2021.100799
Elsner, M. M., Cuo, M. L., Voisin, N., Deems, J. S., Hamlet, A. F., Vano, J. A., et al. (2010). Implications of 21st century climate change for the hydrology of Washington State. *Climatic Change*, *102*(1–2), 225–260. https://doi.org/10.1007/s10584-010-9855-0
Feng, X., Sahoo, A., Arsenault, K., Houser, P., Luo, Y., & Troy, T. J. (2008). The impact of snow model complexity at three CLPX sites. *Journal of Hydrometeorology*, *9*(6), 1464–1481. https://doi.org/10.1175/2008JHM860.1
Foster, L. M., Bearup, L. A., Molotch, N. P., Brooks, P. D., & Maxwell, R. M. (2016). Energy budget increases reduce mean streamflow more than snow–rain transitions: Using integrated modeling to isolate climate change impacts on Rocky Mountain hydrology. *Environmental Research Letters*, *11*(4), 044015. https://doi.org/10.1088/1748-9326/11/4/044015
Griffin, D., & Anchukaitis, K. J. (2014). How unusual is the 2012–2014 California drought? *Geophysical Research Letters*, *41*(24), 9017–9023. https://doi.org/10.1002/2014GL062433.1
Groisman, P. Y., Knight, R. W., Karl, T. R., Easterling, D. R., Sun, B., & Lawrimore, J. H. (2004). Contemporary changes of the hydrological cycle over the contiguous United States: Trends derived from in situ observations. *Journal of Hydrometeorology*, *5*(1), 64–85. https://doi.org/10.1175/1525-7541(2004)005<0064:ccothc>2.0.co;2
Guan, B., Molotch, N. P., Waliser, D. E., Fetzer, E. J., & Neiman, P. J. (2010). Extreme snowfall events linked to atmospheric rivers and surface air temperature via satellite measurements. *Geophysical Research Letters*, *37*(20), L20401. https://doi.org/10.1029/2010gl044696
Gupta, V. K., Soroosh, S., & Yapo, P. O. (1998). Toward improved calibration of hydrological models: Multiple and noncommensurable measures of information. *Water Resources Research*, *34*(4), 751–763. https://doi.org/10.1029/97wr03495
Hale, K. E., Jennings, K. S., Musselman, K. N., Livneh, B., & Molotch, N. P. (2023). Recent decreases in snow water storage in western North America. *Communications Earth & Environment*, *4*(1), 170. https://doi.org/10.1038/s43247-023-00751-3
Hale, K. E., Wlostowski, A. N., Badger, A. M., Musselman, K. N., Livneh, B., & Molotch, N. P. (2022). Modeling streamflow sensitivity to climate warming and surface water inputs in a montane catchment. *Journal of Hydrology: Regional Studies*, *39*, 100976.
Hamlet, A., & Lettenmaier, D. (1999). Columbia River streamflow forecasting based on ENSO and PDO climate signals. *Journal of Water Resources Planning and Management*, *125*(6), 333–341. https://doi.org/10.1061/(ASCE)0733-9496(1999)125:6(333)
Hamlet, A. F., Huppert, D., & Lettenmaier, D. P. (2002). Economic value of long-lead streamflow forecasts for Columbia River hydropower. *Journal of Water Resources Planning and Management*, *128*(2), 91–101. https://doi.org/10.1061/(ASCE)0733-9496(2002)128:2(91)
Hammond, J. C., & Kampf, S. K. (2020). Subannual streamflow responses to rainfall and snowmelt inputs in snow-dominated watersheds of the western United States. *Water Resources Research*, *56*(4), e2019WR026132. https://doi.org/10.1029/2019wr026132
Hammond, J. C., Saavedra, F. A., & Kampf, S. K. (2018). Global snow zone maps and trends in snow persistence 2001-2016. *International Journal of Climatology*, *38*(12), 4369–4383.
Harpold, A., Brooks, P., Rajagopal, S., Heidbuchel, I., Jardine, A., & Stielstra, C. (2012). Changes in snowpack accumulation and ablation in the intermountain west. *Water Resources Research*, *48*(11), W11501. https://doi.org/10.1029/2012WR011949
Hinckley, E., Ebel, B. A., Barnes, R. T., Anderson, R. S., Williams, M. W., & Anderson, S. P. (2012). Aspect control of water movement on hillslopes near the rain-snow transition of the Colorado Front Range. *Hydrological Processes*, *28*(1), 74–85. https://doi.org/10.1002/hyp.9549
Hood, E., Williams, M., & Cline, D. (1999). Sublimation from a seasonal snowpack at a continental, mid-latitude alpine site. *Hydrological Processes*, *13*(12-13), 1781–1797.
Hu, J., Moore, D. J. P., Burns, S. P., & Monson, R. K. (2010). Longer growing seasons lead to less carbon sequestration by a subalpine forest. *Global Change Biology*, *16*(2), 771–783. https://doi.org/10.1111/j.1365-2486.2009.01967.x
Immerzeel, W. W., Lutz, A. F., Andrade, M., Bahl, A., Biemans, H., Bolch, T., et al. (2020). Importance and vulnerability of the world's water towers. *Nature*, *577*(7790), 364–369. https://doi.org/10.1038/s41586-019-1822-y
Jennings, K. S., & Molotch, N. P. (2019). The sensitivity of modeled snow accumulation and melt to precipitation phase methods across a climatic gradient. *Hydrology and Earth System Sciences*, *23*(9), 3765–3786.
Jennings, K. S., Winchell, T. S., Livneh, B., & Molotch, N. P. (2018). Spatial variation of the rain– snow temperature threshold across the Northern Hemisphere. *Nature Communications*, *9*(1), 1148. https://doi.org/10.1038/s41467-018-03629-7
Jeton, A. E., Dettinger, M. D., & Smith, J. L. (1996). Potential effects of climate change on streamflow, eastern and western slopes of the Sierra Nevada, California and Nevada. *US Department of the Interior, US Geological Survey*, *95–4260*, 44.
Kapnick, S., & Hall, A. (2012). Causes of recent changes in western North American snowpack. *Climate Dynamics*, *38*(9–10), 1885–1899. https://doi.org/10.1007/s00382-011-1089-y

Kapnick, S. B., Yang, X., Vecchi, G. A., Delworth, T. L., Gudgel, R., Malyshev, S., et al. (2018). Potential for western US seasonal snowpack prediction. *Proceedings of the National Academy of Sciences of the United States of America*, *115*(6), 1180–1185. https://doi.org/10.1073/pnas.1716760115

Knowles, N., Dettinger, M. D., & Cayan, D. R. (2006). Trends in snowfall versus rainfall in the western United States. *Journal of Climate*, *19*(18), 4545–4559. https://doi.org/10.1175/jcli3850.1

Lehner, F., Wahl, E. R., Wood, A. W., Blatchford, D. B., & Llewellyn, D. (2017). Assessing recent declines in Upper Rio Grande runoff efficiency from a paleoclimate perspective. *Geophysical Research Letters*, *44*(9), 4124–4133. https://doi.org/10.1002/2017gl073253

Liang, X., Lettenmaier, D. P., Wood, E. F., & Burges, S. J. (1994). A simple hydrologically based model of land surface water and energy fluxes for general circulation models. *Journal of Geophysical Research*, *99*(D7), 14415–14428. https://doi.org/10.1029/94jd00483

Livneh, B., & Badger, A. M. (2020). Drought less predictable under declining future snowpack. *Nature Climate Change*, *10*(5), 452–458. https://doi.org/10.1038/s41558-020-0754-8

Livneh, B., Bohn, T. J., Pierce, D. W., Munoz-Arriola, F., Nijssen, B., Vose, R., et al. (2015). A spatially comprehensive, hydrometeorological data set for Mexico, the U.S., and Southern Canada 1950–2013. *Scientific Data*, *2*(1), 150042. https://doi.org/10.1038/sdata.2015.42

Lute, A. C., Abatzoglou, J. T., & Hegewisch, K. C. (2015). Projected changes in snowfall extremes and interannual variability of snowfall in the western United States. *Water Resources Research*, *51*(2), 960–972. https://doi.org/10.1002/2014wr016267

Mahanama, S., Livneh, B., Koster, R., Lettenmaier, D., & Reichle, R. (2012). Soil moisture, snow, and seasonal streamflow forecasts in the United States. *Journal of Hydrometeorology*, *13*(1), 189–203. https://doi.org/10.1175/jhm-d-11-046.1

Mankin, J. S., Viviroli, D., Singh, D., Hoekstra, A. Y., & Diffenbaugh, N. S. (2015). The potential for snow to supply human water demand in the present and future. *Environmental Research Letters*, *10*(11), 114016. https://doi.org/10.1088/1748-9326/10/11/114016

McCabe, G. J., & Clark, M. P. (2005). Trends and variability in snowmelt runoff in the western United States. *Journal of Hydrometeorology*, *6*(4), 476–482. https://doi.org/10.1175/jhm428.1

McNamara, J. P., Chandler, D., Seyfried, M., & Achet, S. (2005). Soil moisture states, lateral flow, and streamflow generation in a semi-arid, snowmelt-driven catchment. *Hydrological Processes: An International Journal*, *19*(20), 4023–4038. https://doi.org/10.1002/hyp.5869

Messerli, B., Viviroli, D., & Weingartner, R. (2004). Mountains of the world: Vulnerable water towers for the 21st century, Ambio Special Report Number 13. *AMBIO: A Journal of the Human Environment*, *13*(13), 29–34. https://doi.org/10.5167/uzh-110516

Mote, P. W., Hamlet, A. F., Clark, M. P., & Lettenmaier, D. P. (2005). Declining Mountain snowpack in western North America. *Bulletin of the American Meteorological Society*, *86*(1), 39–49. https://doi.org/10.1175/BAMS-86-1-39

Mote, P. W., Li, S., Lettenmaier, D. P., Xiao, M., & Engel, R. (2018). Dramatic declines in snowpack in the western US. *Npj Climate and Atmospheric Science*, *1*, 2. https://doi.org/10.1038/s41612-018-0012-1

Musselman, K. N., Addor, N., Vano, J. A., & Molotch, N. P. (2021). Winter melt trends portend widespread declines in snow water resources. *Nature Climate Change*, *11*(5), 418–424. https://doi.org/10.1038/s41558-021-01014-9

Musselman, K. N., Clark, M. P., Liu, C., Ikeda, K., & Rasmussen, R. (2017). Slower snowmelt in a warmer world. *Nature Climate Change*, *7*(3), 214–219. https://doi.org/10.1038/nclimate3225

Neiman, P. J., Schick, L. J., Ralph, F. M., Hughes, M., & Wick, G. A. (2011). Flooding in western Washington: The connection to atmospheric rivers. *Journal of Hydrometeorology*, *12*(6), 1337–1358. https://doi.org/10.1175/2011jhm1358.1

Newman, A. J., Clark, M. P., Sampson, K., Wood, A., Hay, L. E., Bock, A., et al. (2015). Development of a large-sample watershed-scale hydrometeorological data set for the contiguous USA: Data set characteristics and assessment of regional variability in hydrologic model performance. *Hydrology and Earth System Sciences*, *19*(1), 209–223. https://doi.org/10.5194/hess-19-209-2015

Pörtner, H. O., Roberts, D. C., Masson-Delmotte, V., Zhai, P., Tignor, M., Poloczanska, E., & Weyer, N. M. (2019). The ocean and cryosphere in a changing climate. *IPCC Special Report on the Ocean and Cryosphere in a Changing Climate*, 1155.

Raleigh, M. S., & Lundquist, J. D. (2012). Comparing and combining SWE estimates from the SNOW-17 model using PRISM and SWE reconstruction. *Water Resources Research*, *48*(1), W01506. https://doi.org/10.1029/2011wr010542

Regonda, S. K., Rajagopalan, B., Clark, M., & Pitlick, J. (2004). Seasonal cycle shifts in hydroclimatology over the western United States. *Journal of Climate*, *18*(2), 372–384. https://doi.org/10.1175/JCLI-3272.1

Regonda, S. K., Rajagopalan, B., Clark, M., & Pitlick, J. (2005). Seasonal cycle shifts in hydroclimatology over the western United States. *Journal of Climate*, *18*(2), 372–384. https://doi.org/10.1175/jcli-3272.1

Robles, M. D., Hammond, J. C., Kampf, S. K., Biederman, J. A., & Demaria, E. (2021). Winter inputs buffer streamflow sensitivity to snowpack losses in the salt river watershed in the Lower Colorado River Basin. *Water*, *13*(1), 3. https://doi.org/10.3390/w13010003

Safeeq, M., Grant, G. E., Lewis, S. L., & Tague, C. L. (2013). Coupling snowpack and groundwater dynamics to interpret historical streamflow trends in the western United States. *Hydrological Processes*, *27*(5), 655–668. https://doi.org/10.1002/hyp.9628

Staudinger, M., Stahl, K., & Seibert, J. (2014). A drought index accounting for snow. *Water Resources Research*, *50*(10), 7861–7872. https://doi.org/10.1002/2013wr015143

Stewart, I. T. (2009). Changes in snowpack and snowmelt runoff for key mountain regions. *Hydrological Processes*, *23*(1), 78–94.

Stewart, I. T., Cayan, D. R., & Dettinger, M. D. (2004). Changes in snowmelt runoff timing in western North America under a "Business as usual" climate change scenario. *Climatic Change*, *62*(1), 217–232. https://doi.org/10.1023/b:clim.0000013702.22656.e8

Stewart, I. T., Cayan, D. R., & Dettinger, M. D. (2005). Changes toward earlier streamflow timing across western North America. *Journal of Climate*, *18*(8), 1136–1155. https://doi.org/10.1175/JCLI3321.1

Tang, Q., & Lettenmaier, D. P. (2012). 21st century runoff sensitivities of major global river basins. *Geophysical Research Letters*, *39*(3), L06403. https://doi.org/10.1029/2011gl050834

Trujillo, E., & Molotch, N. P. (2014). Snowpack regimes of the western United States. *Water Resources Research*, *50*(7), 5615623–5623. https://doi.org/10.1002/2013WR014753

Trujillo, E., Molotch, N. P., Goulden, M. L., Kelly, A. E., & Bales, R. (2012). Elevation-dependent influence of snow accumulation on forest greening. *Nature Geoscience*, *5*(10), 705–709. https://doi.org/10.1038/ngeo1571

Vano, J. A., & Lettenmaier, D. P. (2012). Hydrologic sensitivities of Colorado River runoff to changes in precipitation and temperature. *Journal of Hydrometeorology*, *13*(3), 932–949. https://doi.org/10.1175/JHM-D-11-069.1

Vano, J. A., Nijssen, B., & Lettenmaier, D. P. (2015). Seasonal hydrologic responses to climate change in the Pacific Northwest. *Water Resources Research*, *51*(4), 1959–1976. https://doi.org/10.1002/2014WR015909

Wieder, W. R., Kennedy, D., Lehner, F., Musselman, K. N., Rogers, K. B., Rosenbloom, N., et al. (2022). Pervasive alterations to snow-dominated ecosystem functions under climate change. *Proceedings of the National Academy of Sciences of the United States of America*, *119*(30). In Press. https://doi.org/10.1073/pnas.2202393119

Wise, E. K. (2012). Hydroclimatology of the US intermountain west. *Progress in Physical Geography*, *36*(4), 458–479. https://doi.org/10.1177/0309133312446538

Woods, R. A. (2009). Analytical model of seasonal climate impacts on snow hydrology: Continuous snowpacks. *Advances in Water Resources*, *32*(10), 1465–1481. https://doi.org/10.1016/j.advwatres.2009.06.011

Yoon, J. H., Wang, S. Y. S., Gillies, R. R., Kravitz, B., Hipps, L., & Rasch, P. J. (2015). Increasing water cycle extremes in California and in relation to ENSO cycle under global warming. *Nature Communications*, *6*, 1–6. https://doi.org/10.1038/ncomms9657

Zhang, D., Cong, Z., Ni, G., Yang, D., & Hu, S. (2015). Effects of snow ratio on annual runoff within the Budyko framework. *Hydrology and Earth System Sciences*, *19*(4), 1977–1992. https://doi.org/10.5194/hess-19-1977-2015